

Inhomogeneous distribution of crosslinks in ion tracks in polystyrene and polysilanes

Shu Seki,* Satoshi Tsukuda, Kensaku Maeda, Yoshinori Matsui, Akinori Saeki, and Seiichi Tagawa†
Institute of Scientific and Industrial Research, Osaka University, 8-1 Mihogaoka, Ibaraki, Osaka 567-0047, Japan
 (Received 11 May 2004; published 22 October 2004)

Gelation in polystyrene, poly(methylphenylsilane), and poly(di-*n*-hexylsilane) induced by irradiation with 30–200 keV Ga, Si, and Au ion beams is examined and compared with that induced by MeV-order ion beams of similar linear energy transfer. The apparent G values of crosslinking (crosslinks per 100 eV absorbed dose) are calculated using the Charlesby-Pinner relationship, and shown to be dramatically lower than for the corresponding MeV ion beams. This decrease is attributed due to the reduced ion track radius and an increase in the density of crosslinking points. The apparent crosslinking G value obtained by the Charlesby-Pinner relationship represents only the crosslinking points contributing to gelation, and other points such as intramolecular crosslinking in the core of the ion track are not counted in the relationship. The total volume of ion tracks is considered to be the most important feature determining the gel fraction produced by the ion beams. A new formulation that provides a good explanation of the gelation of the polymer is proposed, with applicability to ion beams with energy of keV to MeV order.

DOI: 10.1103/PhysRevB.70.144203

PACS number(s): 78.70.-g, 81.07.-b, 41.75.-i, 82.35.Np

I. INTRODUCTION

In recent years, ion implantation of polymers and organic materials has attracted great attention as a means of altering the physical and chemical properties of these materials.^{1,2} Ion bombardment induces structural damage in polymeric materials with enhanced (positive-tone) or reduced (negative-tone) solubility in a solvent.³ Ion irradiation of polymers can be applied to ion beam lithography, and spatial resolutions comparable to electron beam and x-ray lithography can be achieved.⁴

Aoki *et al.*,⁵ Puglisi *et al.*,⁶ Calcagno *et al.*,⁷ and Licciardello *et al.*^{8,9} have reported the effects of ion beam bombardment on polystyrene (PS) as a prototype polymer. Polysilane derivatives have also attracted great interest recently as a new category of polymer materials,^{10,11} and the effects of ion beam irradiation of polysilanes have been reported.^{12,13} The radiation sensitivity of polymers, particularly the G values of chain scission and crosslinking (i.e., number of crosslinks/100 eV of absorbed dose), have been studied for several kinds of ion and electron beams. Aoki *et al.*⁵ examined the relationship between differential G values of crosslinking in PS and stopping power, and proposed some effects of large linear energy transfer (LET; energy deposition of an incident particle per unit length) on crosslinking reactions in PS. Seki *et al.*¹² reported that the G values of crosslinking became larger as the LET of radiation increases, and attributed these phenomena to “LET effects.” The ion track radius is also an important parameter because the energy of the incident ion is deposited in a defined area, and the spatial distribution of energy deposited by charged ions has been suggested to play a significant role in chemical reactions.^{14–16} Seki *et al.*,^{16,17} Koizumi *et al.*^{18,19} and Licciardello and Puglisi^{8,9} elucidated the relationship between the radiation effects of ion beam bombardment and the chemical core radius in an ion track. The crosslinking reactions within the defined area in particular have a cylindrical nanostructure, and our group has reported nanowire formation based on this feature through MeV-order ion beam irradiation

of thin films of several kinds of crosslinking-type polymers.^{20–23}

In this paper, the crosslinking G values induced by keV-order ion beams are compared with those resulting from MeV-order ion beam irradiation. The relationship between the crosslinking G value and the chemical core radius in an ion track is discussed, and a new formulation of polymer gelation induced by ion beams is proposed.

II. EXPERIMENT

Polystyrene (PS: $M_n=1.0 \times 10^4$, $M_w/M_n=1.04$) was purchased from Aldrich Chemical Co. Ltd., and used without further purification. Poly(methylphenylsilane) (PMPS) was prepared by reaction of methylphenyldichlorosilane with sodium in refluxing toluene.²⁴ Poly(di-*n*-hexylsilane) (PDHS) was prepared by reaction of di-*n*-hexyldichlorosilane with sodium in refluxing toluene.²⁵ Chlorosilane was purchased from Shin-Etsu Chemical Inc. and distilled prior to use. Fractional precipitations were repeated more than 5 times to suppress polydispersity. The molecular weights of PMPS and PDHS samples were measured by gel permeation chromatography (GPC) with tetrahydrofuran (THF) as the eluent. The PMPS and PDHS samples had molecular weights of $M_n=1.1 \times 10^4$ and 4.8×10^4 , $M_w/M_n < 1.2$, respectively, as determined by polystyrene calibration standards.

The polymer samples were dissolved in toluene and spin coated on Si wafers to thicknesses of 0.03–0.1 μm . The samples were then irradiated with keV-order ion beams in a vacuum chamber ($< 10^{-8}$ Torr) at room temperature using a JEOL JIBL-100L or Seiko Instruments Inc. SMI-2050 focused ion beam microscope. After irradiation, all samples were developed in toluene for 2 min. The irradiated part of the film, where gel was generated, was insoluble in toluene. Films were dried under vacuum for 30 min and measured using a surface profiler (SE-2300, Kosaka Laboratory) and by atomic force microscopy (AFM: SPI-3800, Seiko Instru-

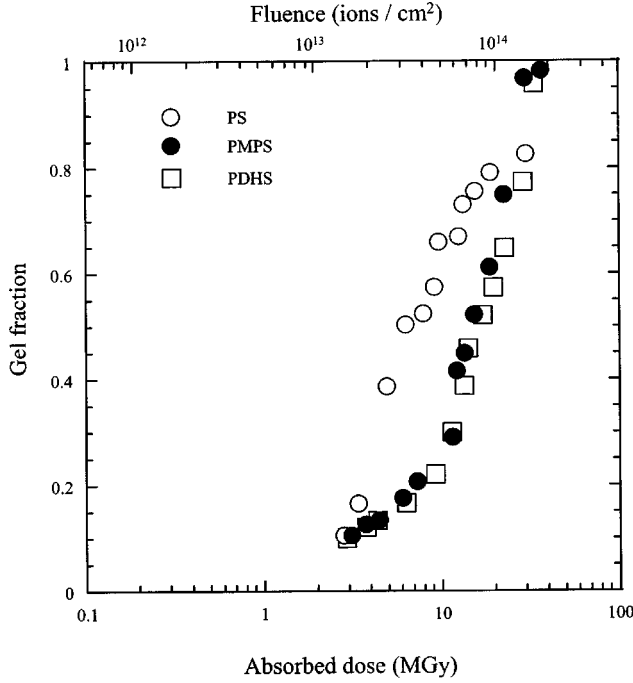


FIG. 1. Absorbed dose dependence of gel fraction for 100 keV Ga ion beam irradiation.

ments. Inc.). The gel fraction was defined as the ratio of the thickness after irradiation to that before.

The loss of kinetic energy of ions traversing the polymer films was estimated using SRIM 2000 code.²⁶ The apparent crosslinking G values were calculated by the Charlesby-Pinner equation. Infrared (IR) spectra were measured for the irradiated PMPS sample using a Fourier transform IR (FT-IR) spectrometer (Spectrum-2000, Perkin Elmer).

III. RESULTS AND DISCUSSION

A. Calculation and comparison of crosslinking G values

After irradiation of PS, PMPS, and PDHS films with 100 keV Ga ion beams, the gelation of the polymers was observed. Figure 1 plots the gel fraction of the polymers against the absorbed dose. According to the statistical theory of crosslinking and scission of the polymers induced by radiation, the behavior of gelation can be described by the following equation (Charlesby-Pinner relationship),²⁷⁻²⁹

$$s + s^{1/2} = p/q + \frac{m}{q} M_n D, \quad s = 1 - g, \quad (1)$$

$$D = \frac{\text{LET}}{\rho} n e, \quad (2)$$

where p is the probability of scission, q is the probability of crosslinking, s is the sol fraction, g is the gel fraction, m is the molecular weight of the unit monomer, M_n is the number average molecular weight before irradiation, D is the absorbed dose, e is the charge of an electron, n is the fluence, and ρ is the density of target materials. The G value is related to the values of p and q as follows:

$$G(x) = 4.8 \times 10^3 q, \quad (3)$$

$$G(s) = 9.6 \times 10^3 p, \quad (4)$$

where $G(x)$ and $G(s)$ are the G values of crosslinking and main-chain scission, respectively. Radiation-induced crosslinking behavior has been formulated by many groups considering the molecular weight distribution and/or molecular stiffness of the polymer target. The problem of the change in the molecular weight distribution with irradiation was solved by Saito^{30,31} and Inokuti.^{32,33} In their theory, molecular weight distributions are expanded by the Poisson and/or Schulz-Zimm distributions, and the changes in the distribution due to simultaneous reactions of main-chain scission and crosslinking are traced analytically. However in the present case, the molecular weight distributions of the target polymers are reasonably controlled to be less than 1.2, and the initial distributions are predicted not to play a crucial role in gelation. The effects of molecular stiffness on the crosslinking reactions were considered by Zhang *et al.* as follows:³⁴

$$D(s + s^{1/2}) = \frac{2}{q u_w} + \frac{\alpha}{q} D^\beta, \quad (5)$$

$$\beta = 0.002 T_g + 0.206, \quad (6)$$

where α is a constant, T_g is the glass transition temperature of the target polymers, and u_w is the initial weight average degree of polymerization. The simultaneous change in the molecular weight distribution due to radiation-induced reactions also results in a nonlinearity of the Charlesby-Pinner relationship. The following equations are therefore proposed to extend the validity of the relationship by introducing a deductive distribution function of molecular weight on the basis of an arbitrary distribution:³⁵

$$s + s^{1/2} = p/q + \frac{(2 - p/q)(D_v - D_g)}{(D_v - D)}, \quad (7)$$

$$D_v = 4 \left(\frac{1}{u u_n} - \frac{1}{u_w} \right) / 3q, \quad (8)$$

where D_g is the gelation dose, and u is the degree of polymerization. The values of T_g for PS and PMPS are 375 and 393 K, respectively, whereas PDHS exhibits a liquid crystalline transition temperature at 313 K. This suggests that Eq. (5) is not effective for comparing the crosslinking G values obtained for PS and PMPS, despite the stronger effect on the value of PDHS. The persistence length of the polymer chains are almost identical [PS, 0.9 nm;³⁶ PMPS, 1.1 nm (Ref. 37)], directly reflecting the molecular stiffness of the target polymers and supporting the consistency of Eqs. (1) and (5) for the determination of G values in PS and PMPS, although Eq. (1) may give misleading values for PDHS (persistence length, 3.0 nm). The values of $G(x)$ for PS and PMPS were calculated based using both Eqs. (1) and (7) for 100 keV Ga ion beams. The equations give similar values of $G(x)$ for PS (0.09 and 0.11) and PMPS (0.032 and 0.036), suggesting that

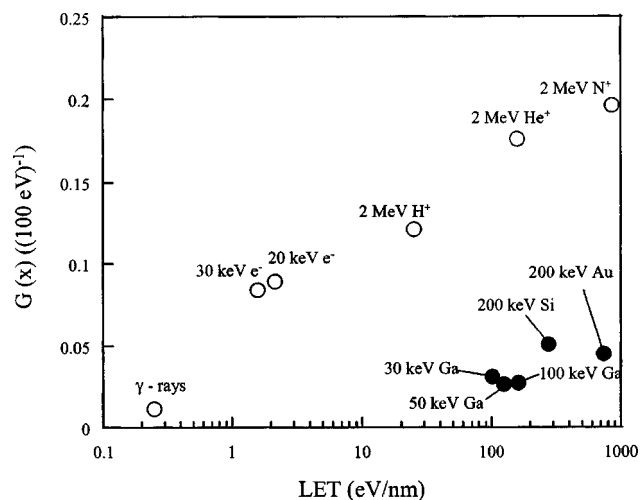


FIG. 2. Semilogarithmic plot of calculated $G(x)$ vs LET.

the Charlesby-Pinner relationship is sufficiently linear in the high-dose region, as shown in Fig. 1.

On the basis of the Charlesby-Pinner relationship, the apparent G values for 30, 50, and 100 keV Ga, 200 keV Si, and 200 keV Au ion beams are compared with those for MeV order ion beams of the same LET in Fig. 2 and Table I.^{12,13} It is clear that the apparent crosslinking G values for keV-order ion beams are clearly lower than those for MeV-order ion beams. All the low-energy ion beams give values of $G(x) \sim 0.03$ – 0.04 , one order of magnitude lower than those observed for high-energy ion beams with similar LET.

B. IR spectra for PMPS

The IR spectra for PMPS films changed due to irradiation with 100 keV Ga ion beams, as shown in Fig. 3. Relatively sharp features in the spectra became broader upon irradiation. The broadening of peak (4) may be due to oxidation, which is likely for the siloxane structure. An increase in the broad signal at 800 cm^{-1} reflects the formation of a three-dimensional Si-C structure. The intensity of peaks (2) and (3) and decreased after irradiation, indicating the dissociation of methyl and phenyl substituents from the polymer backbone as supported by the decrease in the intensity of peak (1), which correspond to the C-H stretching of methyl and phenyl substituents. An increase in the band at 2000 cm^{-1} is ascribed to an increase in the number of Si-H bonds as a result of main-chain scission leaving hydrogen-terminated chain ends. These changes in the IR spectra after irradiation with a 100 keV Ga ion beam are similar to those induced by irradiation with a 2 MeV He ion beam as reported previously.¹² Hence, the reaction scheme for 100 keV Ga ion-beam irradiation is considered to be analogous of that for a 2 MeV He ion beam, suggesting that the drastic decrease in apparent $G(x)$ is not caused by the difference in the radiation-induced reactions.

C. Calculation and comparison of ion track radius

The following equation describes the ratio of the total area covered by the cross sections (σ) of the chemical core in ion tracks:

TABLE I. Crosslinking G values for PMPS, PDHS, and PS irradiated with 100 keV Ga and 2 MeV He ion beams.

	$G(x)$ for 100 keV Ga	$G(x)^a$ for MeV-order ion beams
PMPS	0.032	0.15
PDHS	0.01	0.40
PS	0.09	1.8

^a $G(x)$ is scaled by previous studies for PMPS (Ref. 12), PDHS (Ref. 17), and PS (Ref. 5).

$$S_{n+1} = S_n + \sigma[1 - (S_n/S)], \quad (9)$$

where S and S_n denote the total volume of the polymer films, and the total volume of the chemical cores. As the polymer films used in this experiment were sufficiently thin to allow the ion tracks to be regarded as cylindrical, S_n/S can be estimated as the ratio of the area covered by the chemical cores to that of the film surface. Equation (9) leads to the following expression:

$$S_n = S - (1 - \sigma/S)^n. \quad (10)$$

For $S=1\text{ cm}^2$, this becomes

$$S_n = 1 - (1 - \sigma)^n, \quad (11)$$

$$1 - S_n = (1 - \sigma)^n, \quad (12)$$

where n is the fluence per cm^2 .

Equation (12) then gives the following forms:^{38,39}

$$1 - S_n = \exp(-n\sigma), \quad \sigma \ll 1, \quad (13)$$

$$1 - S_n = 1 - n\sigma, \quad n\sigma \ll 1. \quad (14)$$

Figures 4(a) and 4(b) show the increase in gel formation with D (MGy) and the variation in the sol fraction against n (ions/ cm^2). The sol fraction decreases exponentially with fluence of the 2 MeV He ion beam, in contrast to the monotonic decrease seen for the 100 keV Ga ion beam, attributable to the minimal overlap of the chemical cores at these fluences. Using Eqs. (9) and (10), the experimental data can be fitted for the sol fraction to give the sections of the chemical core for 2 MeV He and 100 keV Ga ion beams. The calculated radii for PMPS are 3.5 nm for the 2 MeV He ion beam and 0.5 nm for the 100 keV Ga ion beam, and 4.2 nm and 0.7 nm for PDHS, respectively. The values are in good agreement with those reported by Seki *et al.*^{16,17} and Papaleo *et al.*³⁹ The experimental results are also supported by theoretical studies on ion tracks and chemical core radii, which have shown that the radius of the penumbra area for keV-order ion beams is very small in comparison with that of MeV-order ion beams, as described below.¹⁴

D. Gelation and track radius

The density of reactive intermediates controls the crosslinking reaction in PMPS, as supported by the presence of a LET threshold (ca. 10 eV/nm), to afford a polymer gel.

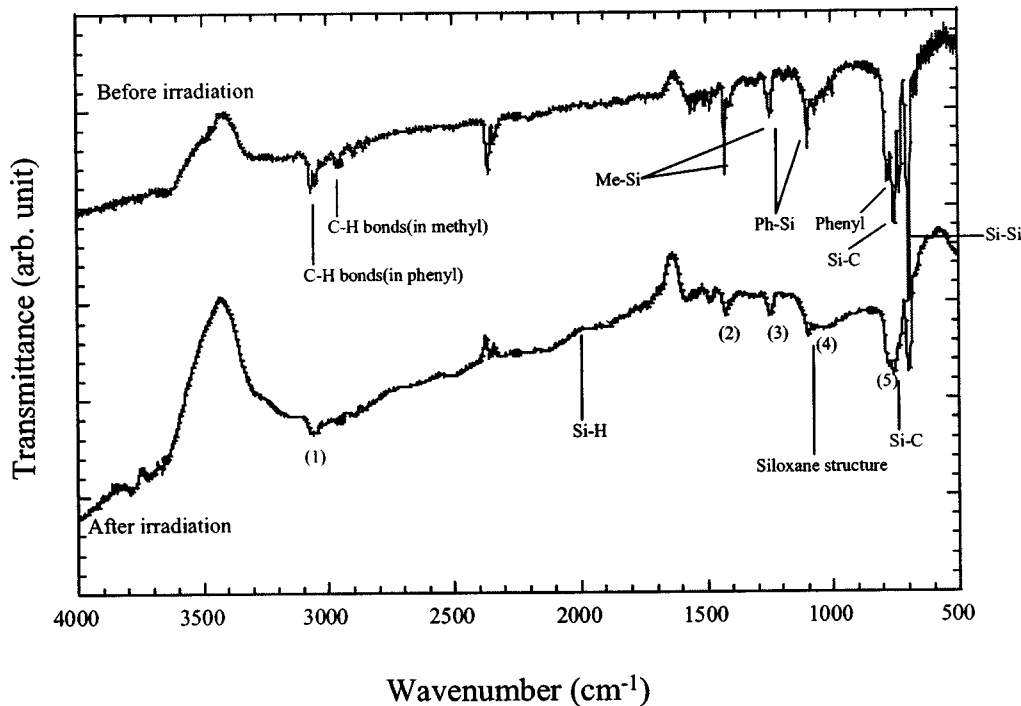


FIG. 3. IR spectra of PMPS before and after irradiation with 100 keV Ga ion beam at 18.8 MGy (9.4×10^{13} ions/cm²).

Seki *et al.* reported that the apparent crosslinking reactions are mainly promoted by side-chain dissociated silyl radicals, and found that the predominant reaction is determined by the radical concentration in the ion tracks.^{17,40–42} Thus, the distribution of crosslinking points in an ion track is expected to reflect the radial energy density, where ρ_{cr} is the critical energy density for the predominance of crosslinking in PMPS. The present values of radii are larger than that the core size suggested by theoretical considerations.¹⁴ According to the theory, the following formulas give the coaxial energy in an ion track:^{43,44}

$$\rho_c = \frac{LET}{2} [\pi r_c^2]^{-1} + \frac{LET}{2} \left[2\pi r_c^2 \ln \left(\frac{e^{1/2} r_p}{r_c} \right) \right]^{-1}, \quad r \leq r_c, \quad (15)$$

$$\rho_p(r) = \frac{LET}{2} \left[2\pi r^2 \ln \left(\frac{e^{1/2} r_p}{r_c} \right) \right]^{-1}, \quad r_c < r \leq r_p, \quad (16)$$

where ρ_c is the deposited energy density in the core area, r_c and r_p are the radii of core and penumbra area, and e is an exponential factor. The values of ρ_c for irradiation with 100 keV Ga and 2 MeV He ion beams are estimated to be 1.3×10^7 and 3.3×10^2 , respectively. Figure 5 shows the ion track models for these two ion beams. At the center part of the ion tracks, the number of crosslinking points is predicted to be much larger than the number needed to form polymer gels by irradiation with a 100 keV Ga ion beam. However, the energy deposited below ρ_{cr} within the ion track by the 100 keV Ga ion beam is much lower than that by the 2 MeV He ion beam, and the volume of gel is much lower, indicating lower apparent crosslinking G values. Thus, in irradiation with an ion beam, the size of the chemical track is re-

sponsible for the gel fraction. The cylindrical shape of the chemical core can also be visualized by AFM, as shown in Fig. 6. The polymer molecules in the chemical cores certainly become insoluble, and remain on the substrate after removal of the nonirradiated part by solvent washing.

Equations (15) and (16), however, are based on a Born approximation for the collision of incident particles with target atoms and/or electrons.⁴⁵ It is apparent that this approximation is not adequate for collision events involving incident particles of lower velocity (v) than the orbital velocity of electrons in the target material (v_0). The value of v_0 in the present target materials is given approximately by

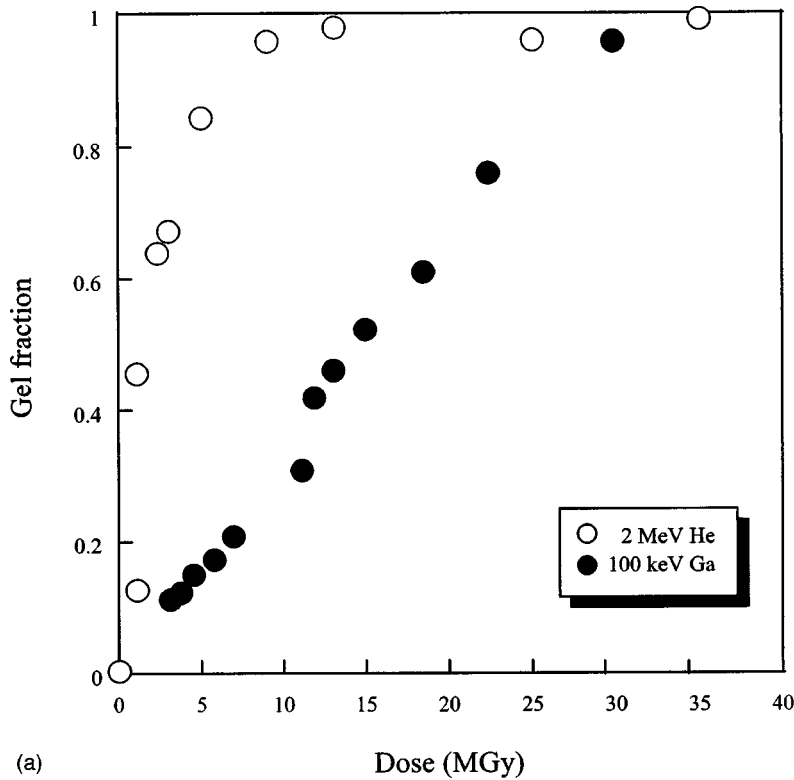
$$v_0 = \frac{e^2}{\hbar} Z^{2/3}, \quad (17)$$

where Z is the average atomic number of the target. The value of v_0 for the present target is 1.6×10^7 ms⁻¹, which is almost comparable to the value of v for 100 keV Ga ions (4.4×10^6 ms⁻¹), suggesting that it is necessary to use the extended theory for stopping power calculations. A universal model of the stopping power (S) for incident charged particles was formulated by Lindhard *et al.* as follows:⁴⁶

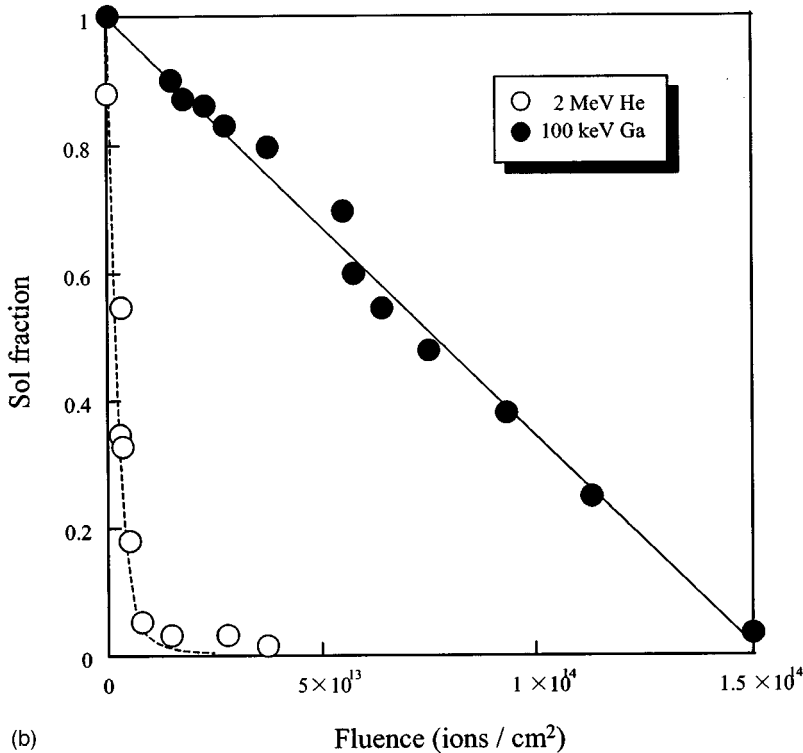
$$S = \frac{4\pi Z^2 e^4}{m_e v^2} NL, \quad (18)$$

$$L = \frac{1}{\pi \omega_p} \text{Im} \left[\int_0^\infty \frac{dk}{k} \int_{-kv}^{kv} \omega d\omega \left(\frac{1}{\kappa(k, \omega)} \right) \right], \quad (19)$$

where m_e is the mass of an electron, N is the number of electrons per unit volume, κ is the dielectric constant of the



(a)



(b)

FIG. 4. (a) Relationship between gel fraction and absorbed dose for 2 MeV He ion beam and 100 keV Ga ion beam irradiation to PMPS. (b) Relation between sol fraction and fluence for 2 MeV He ion beam and 100 keV Ga ion beam irradiation to PMPS.

target, and ω_p is the plasma oscillation frequency, which is given by

$$\omega_p^2 = \frac{4\pi Ne^2}{m_e}. \quad (20)$$

Based on Eqs. (18)–(20), numerical integration gives an average excitation energy (E_{av}) for the present target material

(PMPS, density = 1.05 g cm⁻³) and 100 keV Ga ion beam of ca. 8 eV. This value is almost equivalent to the ionization potential of PMPS (5.5 eV), indicating an ultralow range of ejected electrons from the molecules and no penumbra area in the track of the 100 keV Ga ion beam. Firsov *et al.* also suggested the following equations for estimating the energy loss of incident low-energy particles in a collision event:⁴⁷

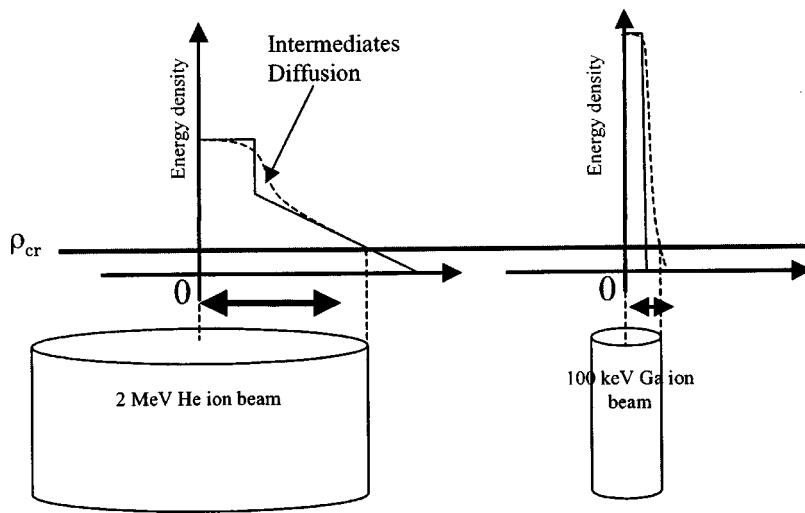


FIG. 5. Schematic energy diagram of energy density for 2 MeV He ion beam and 100 keV Ga ion beam.

$$\Delta E = E_R \frac{0.7(Z_1 + Z_2)^{5/3}(ve^2/\hbar)}{1 + 0.16(Z_1 + Z_2)^{1/3}(\mu/a_B)}, \quad (21)$$

where E_R is the Rydberg energy, a_B is the Bohr radius, Z_1 and Z_2 are the mass of the incident and target atoms, and μ is the collision factor. This equation also gives a value of $\Delta E \sim 10$ eV in the present case.

The present results illustrate that σ (chemical core radius) is determined more by the diffusion of reactive intermediates from the center part of the tracks than the initial spatial distribution of the deposited energy by secondary electrons in the case of incident ions with velocity comparable to v_0 (Fig. 5). This is also supported by the IR spectra, which indicated Si-C ceramic formation upon irradiation with 100 keV Ga ion beams. The conversion ratio reached 40%–50% at 40 MGy, where the gel fraction reaches 100%. This suggests that an extremely high energy density at the center of the ion track causes the formation of an Si-C ceramic structure rather than a simple crosslinking of polymer molecules.⁴⁸ We previously proposed the following simple forms of Eq. (13) to trace the gel fraction formed by ion beams having a relatively large radial distribution in an ion track:¹⁷

$$g = 1 - \exp[-n\pi(r' + \delta r')^2], \quad (22)$$

$$r_{cc} = r' + \delta r'. \quad (23)$$

Here, r_{cc} is the overall radius of the chemical core, r' is the chemical core radius determined by the initial energy density of deposited energy in an ion track and the size of the target

molecules, and $\delta r'$ is the differential radius determined by the diffusion of reactive intermediates and the reaction rate constants. On the basis of the very low E_{av} and ΔE given by Eqs. (18)–(21), the obtained values of σ in the present study suggest a $\delta r'$ value of 0.5–0.7 nm. Despite the large difference in the structure and the reactivity of PS, PDHS, and PMPS, the values of $\delta r'$ for the two targets are almost identical, suggesting that the values can be regarded as a constant. For gel formation in a polymer system, it is necessary to introduce one crosslink per polymer molecule. Assuming a sole contribution from the crosslinking reactions in the chemical core, ρ_{cr} is given by

$$\rho_{cr} = \frac{100\rho A}{G(x)mk}, \quad (24)$$

where A is Avogadro's number, and k is the degree of polymerization. Substitution of $\rho_p(r)$ in Eq. (16) with ρ_{cr} gives the following requirement for r' :

$$r'^2 = \frac{LET \cdot G(x)mk}{400\pi\rho A} \left[\ln\left(\frac{e^{1/2}r_p}{r_c}\right) \right]^{-1}. \quad (25)$$

Equations (23) and (25) provide good interpretations of the values of r_{cc} reported by direct AFM observation^{20,22,23} and by tracing the gel fraction^{16,17,19,21} for several kinds of polymer targets and high-energy (MeV order) ion beams with sufficiently large penumbra area ($r_p > \sim 10$ nm). The predominant factor determining the chemical core size is therefore chemical reactions at the boundary surface of the

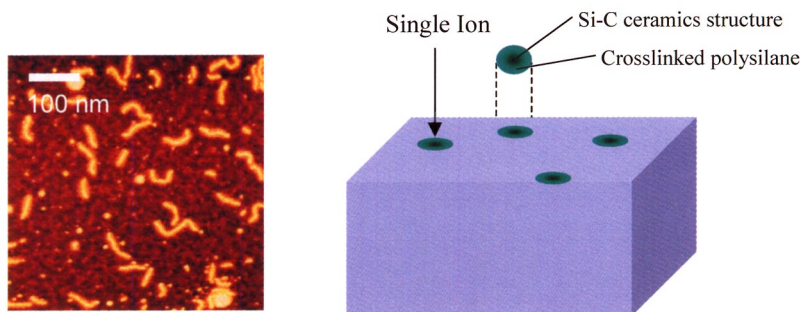


FIG. 6. AFM image of chemical cores formed in 100 nm thick PMPS thin film by irradiation with a 2 MeV He beam. The structures are observed after 2 min washing with benzene to completely dissolve PMPS.

core, even in the case of low-energy ion beams. Thus, we believe that ion beams with a variety of energies from keV to GeV are suitable for single-particle fabrication with subnanometer-scale spatial resolution.

IV. CONCLUSIONS

The apparent crosslinking G values of keV-order ion beams were calculated and compared with those of MeV-order ion beams, and shown to be dramatically lower. As the ion track radius was found to be smaller, this decrease in crosslinking G value does not appear to be due to differences in the reaction mechanism, with the volume of gel simply decreasing proportionally to the shortening of the ion track radius. The chemical core sizes formed by keV-order ($v \sim v_0$) ion beams were found to be determined by the diffu-

sion of reactive intermediates from the center part of the tracks, although the chemical reactions at the boundary surface of the core represents the dominant factor determining the chemical core sizes even for keV-order ion beams. A new formulation that provides a good explanation of the chemical core radius was also proposed. These results demonstrate that a well-defined chemical core produced by an appropriate ion beam may be applicable for the fabrication of single particles.

ACKNOWLEDGMENTS

The authors thank Professor H. Shibata, Graduate School of Engineering, Kyoto University and Dr. Y. Kunimi of the ISIR, Osaka University for valuable discussion. This work was supported in part by a Grant-in-Aid for scientific research from the Japan Society for the Promotion of Science.

*Author to whom correspondence should be addressed; Email address: seki@sanken.osaka-u.ac.jp

†Author to whom correspondence should be addressed; Email address: tagawa@sanken.osaka-u.ac.jp

¹H. Ryssel, K. Habberger, and H. Kranz, *J. Vac. Sci. Technol.* **19**, 1358 (1981).

²T. M. Hall, A. Wagner, and L. F. Thompson, *J. Vac. Sci. Technol.* **16**, 1889 (1979).

³I. Adesida, *Nucl. Instrum. Methods Phys. Res.* **209/210**, 79 (1983).

⁴W.L. Brown, T. Venkatesan, and A. Wagner, *Nucl. Instrum. Methods Phys. Res.* **191**, 157 (1981).

⁵Y. Aoki, N. Kouchi, H. Shibata, S. Tagawa, Y. Tabata, and S. Imamura, *Nucl. Instrum. Methods Phys. Res. B* **33**, 799 (1988).

⁶O. Puglisi and A. Licciardello, *Nucl. Instrum. Methods Phys. Res. B* **19/20**, 865 (1987).

⁷L. Calcagno and G. Foti, *Appl. Phys. Lett.* **51**, 907 (1987).

⁸A. Licciardello and O. Puglisi, *Nucl. Instrum. Methods Phys. Res. B* **32**, 131 (1988).

⁹A. Licciardello, O. Puglisi, L. Calcagno, and G. Foti, *Nucl. Instrum. Methods Phys. Res. B* **46**, 338 (1990).

¹⁰R. D. Miller and J. Michl, *Chem. Rev. (Washington, D.C.)* **89**, 1359 (1989).

¹¹R. D. Miller, *Advances in Chemistry Series 224* (American Chemical Society, Washington DC, 1990), p. 413.

¹²S. Seki, H. Shibata, H. Ban, K. Ishigure, and S. Tagawa, *Radiat. Phys. Chem.* **48**, 539 (1996).

¹³S. Seki, K. Kanzaki, Y. Yoshida, H. Shibata, K. Asai, S. Tagawa, and K. Ishigure, *Jpn. J. Appl. Phys., Part 1* **36**, 5361 (1997).

¹⁴J.L. Magee and A. Chatterjee, in *Kinetics of Nonhomogenous Processes*, edited by G. R. Freeman (Wiley, New York, 1987), Chap. 4, p. 171.

¹⁵T. Tombello, *Nucl. Instrum. Methods Phys. Res. B* **2**, 555 (1984).

¹⁶S. Seki, K. Kanzaki, Y. Kunimi, Y. Yoshida, H. Kudoh, M. Sugimoto, T. Sasuga, S. Tagawa, and H. Shibata, *Radiat. Phys. Chem.* **50**, 423 (1997).

¹⁷S. Seki, K. Maeda, Y. Kunimi, S. Tagawa, Y. Yoshida, H. Kudoh, M. Sugimoto, Y. Morita, T. Seguchi, T. Iwai, H. Shibata, K.

Asai, and K. Ishigure, *J. Phys. Chem. B* **103**, 3043 (1999).

¹⁸H. Koizumi, T. Ichikawa, H. Yoshida, H. Shibata, S. Tagawa, and Y. Yoshida, *Nucl. Instrum. Methods Phys. Res. B* **117**, 269 (1996).

¹⁹H. Koizumi, M. Taguchi, Y. Kobayashi, and T. Ichikawa, *Nucl. Instrum. Methods Phys. Res. B* **179**, 530 (2001).

²⁰S. Seki, K. Maeda, S. Tagawa, H. Kudoh, M. Sugimoto, Y. Morita, and H. Shibata, *Adv. Mater. (Weinheim, Ger.)* **13**, 1663 (2001).

²¹S. Seki, S. Tsukuda, Y. Yoshida, T. Kozawa, S. Tagawa, M. Sugimoto, and S. Tanaka, *Jpn. J. Appl. Phys., Part 1* **42**, 4159 (2003).

²²S. Tsukuda, S. Seki, S. Tagawa, M. Sugimoto, A. Idesaki, and S. Tanaka, *J. Photopolym. Sci. Technol.* **16**, 433 (2003).

²³S. Tsukuda, S. Seki, S. Tagawa, M. Sugimoto, A. Idesaki, S. Tanaka, and A. Ohshima, *J. Phys. Chem. B* **108**, 3407 (2004).

²⁴S. Seki, Y. Yoshida, S. Tagawa, and K. Asai, *Macromolecules* **32**, 1080 (1999).

²⁵S. Seki, Y. Koizumi, T. Kawaguchi, H. Habara, and S. Tagawa, *J. Am. Chem. Soc.* **126**, 3521 (2004).

²⁶J. F. Ziegler, J. P. Biersack, and U. Littmaek, *The Stopping and Range of Ions in Solids*, (Pergamon, New York, 1985).

²⁷A. Charlesby, *Proc. R. Soc. London, Ser. A* **222**, 60 (1954).

²⁸A. Charlesby, *Proc. R. Soc. London, Ser. A* **224**, 120 (1954).

²⁹A. Charlesby and S. H. Pinner, *Proc. R. Soc. London, Ser. A* **249**, 367 (1959).

³⁰O. Saito, *J. Phys. Soc. Jpn.* **13**, 1451 (1958).

³¹O. Saito, *J. Phys. Soc. Jpn.* **14**, 798 (1959).

³²M. Inokuti, *J. Chem. Phys.* **33**, 1607 (1960).

³³M. Inokuti, *J. Chem. Phys.* **38**, 2999 (1963).

³⁴Y. F. Zhang, X. W. Ge, and J. Z. Sun, *Radiat. Phys. Chem.* **35**, 163 (1990).

³⁵K. Olejniczak, J. Rosiak, and A. Charlesby, *Radiat. Phys. Chem.* **37**, 499 (1991).

³⁶D. Schrader, in *Polymer Data Handbook*, edited by J. Brandrup, E.H. Immergut, and E.A. Grulke (Wiley, New York, 1999), Chap. 5, p. 91.

³⁷S. Seki, Y. Matsui, Y. Yoshida, S. Tagawa, J.R. Koe, and M.

- Fujiki, J. Phys. Chem. B **106**, 6849 (2002).
- ³⁸M. Salehpour, P. Hakansson, and B. Sundqvist, Nucl. Instrum. Methods Phys. Res. B **2**, 752 (1984).
- ³⁹R. M. Papaleo, A. Hallen, B. U. R. Sundqvist, L. Farenzena, R. P. Livi, M. A. de Araujo, and R. E. Johnson, Phys. Rev. B **53**, 2303 (1996).
- ⁴⁰G. N. Taylor, W. W. Wolf, and J. M. Moran, J. Vac. Sci. Technol. **19**, 872 (1981).
- ⁴¹S. Seki, K. R. Cromack, A. D. Trifunac, Y. Yoshida, S. Tagawa, K. Asai, and K. Ishigure, J. Phys. Chem. B **102**, 8367 (1998).
- ⁴²S. Seki, S. Tagawa, K. Ishigure, K. R. Cromack, and A. D. Trifunac, Radiat. Phys. Chem. **47**, 217 (1996).
- ⁴³J. L. Magee and A. Chatterjee, J. Phys. Chem. **84**, 3529 (1980).
- ⁴⁴A. Chatterjee and J. L. Magee, J. Phys. Chem. **84**, 3537 (1980).
- ⁴⁵M. Inokuti, Rev. Mod. Phys. **43**, 297 (1971).
- ⁴⁶J. Lindhard and M. Scharff, Phys. Rev. **124**, 128 (1961).
- ⁴⁷O.B. Firsov, Sov. Phys. JETP **9**, 1076 (1959).
- ⁴⁸T. Venkatesan, T. Wolf, D. Allara, X. Wilkens, and G. N. Taylor, Appl. Phys. Lett. **43**, 934 (1983).